Smart Structures and Systems, *Vol. 28, No. 4 (2021) 499-513*
https://doi.org/10.12989/sss.2021.28.4.499

Influence of porosity on the hygro-thermo-mechanical bending response of an AFG ceramic-metal plates using an integral plate model

Mohammed A. Al-Osta [1,4], Hayat Saidi [2], Abdelouahed Tounsi*[1,2,3], S.U. Al-Dulaijan [1], M.M. Al-Zahrani [1], Alfarabi Sharif [1] and Abdeldjebbar Tounsi [2]

[1] *Department of Civil and Environmental Engineering, King Fahd University of Petroleum & Minerals, 31261 Dhahran, Eastern Province, Saudi Arabia*
[2] *Material and Hydrology Laboratory, University of Sidi Bel Abbes, Faculty of Technology, Civil Engineering Department, Algeria*
[3] *YFL (Yonsei Frontier Lab), Yonsei University, Seoul, Korea*
[4] *Interdisciplinary Research Center for Construction and Building Materials, KFUPM, Dhahran, Saudi Arabia*

(*Received September 16, 2020, Revised June 29, 2021, Accepted July 29, 2021*)

Abstract. In this project, the hygro-thermo-mechanical bending behavior of perfect and imperfect advanced functionally graded (AFG) ceramic-metal plates is analytically investigated using an integral plate model for the first time. The plate is assumed to be supported by a two-parameter elastic foundation. Because of the technical problems encountered in the manufacture of AFG, porosities and micro-voids can occur in AFG specimens, which can result in reduced density and strength of materials. Thus, due to the presence of porosity, a modified rule of mixture is adopted to predict the material properties of the AFG plates. The governing equations are deduced by adopting the "principle of virtual work" and an integral plate model. The analytical Navier's method is considered to solve the obtained differential equations for simply supported AFG porous plate. The results obtained are checked by comparing them for non-porous and porous AFG plates with those available in the open literature. Finally, this work will help us to design advanced functionally graded materials to ensure better durability and efficiency for hygro-thermal environments.

Keywords: advanced functionally graded materials; elastic foundation; hygro-thermo-mechanical loading; integral plate theory; porosity

1. Introduction

Advanced functionally graded materials (AFGMs) are prepared from a mixture of ceramic and metal with a requested variation in the volume fractions of these two materials between the two external faces of any structure. Mechanical properties like Young's modulus, Poisson's ratio, the shear modulus, mass density, and both thermal and moisture expansions, change continuously and smoothly within the AFG plates. These components are generally based on the technical alloys of "aluminum, titanium, magnesium, steel, copper, tungsten", etc., as well as advanced structural ceramics such as "zirconia, alumina, silicon-carbide and tungsten-carbide" (Birman and Byrd 2007, Carrera *et al*. 2008, Yang *et al*. 2012, Carrera *et al*. 2011, Attia 2017, Faleh *et al*. 2018, Madenci 2019, Sayyad and Ghumare 2019, Fesharaki and Roghani 2019, Boulal *et al*. 2020, Si *et al*. 2020, Fenjan *et al*. 2020, Yuan *et al*. 2020, Zhu *et al*. 2020, Jena *et al*. 2020, Vinyas 2020, Heidari *et al*. 2020, Dehshahri *et al*. 2020). Studies for thermal analysis on FG plates were discussed (Sofiyev 2011, Duc and Tung 2011, Kasaeian *et al*. 2011, Wang and Shen 2013). The subject of the thermoelastic analysis of plates and shells has always attracted the attention of many researchers. Mehar and Panda (2017a) presented a numerical study of nonlinear thermo-mechanical deflection of FGCNT reinforced doubly curved composite shell panel under different mechanical loads. In addition, Mehar and Panda (2017b) investigated the thermoelastic response of FG-CNT reinforced shear deformable composite plate under various loadings.

The simplest and oldest model to define the interaction between the AFG plate and the foundation is the one-parameter or Winkler model (Winkler 1867). By including a shear spring to the model of Winkler, this version improved the Pasternak model (Han and Liew 1997, Shen 2000, Yas and Tahouneh 2012, Avcar and Mohammed 2018). On the basis of the literature, it seems that many researchers have employed the classical plate theory (Chucheepsakul and Chinnaboon 2002, Civalek 2007a) and the theories of shear deformation, such as the first higher-order shear deformation theories and the "3D elasticity theory" as presented in (Shen *et al*. 2001, Xiang 2003, Zhou *et al*. 2004, Abdalla and Ibrahim 2006, Ozgan and Daloglu 2007, Civalek 2007b).

For FG imperfect plates, many researchers are interested in the dynamic investigation of FG imperfect (porous) structures (Rezaei and Saidi 2015, Behravan Rad and Shariyat 2015, Rezaei and Saidi 2016, Shafiei *et al*. 2016, Chen *et al*. 2016, Shafiei *et al*. 2017, Wu *et al*. 2018, Thanh *et al*. 2021), the analysis of buckling and post-buckling

*Corresponding author, Professor,
E-mail: tou_abdel@yahoo.com

ISSN: 1738-1584 (Print), 1738-1991 (Online)

(Khorshidvand *et al*. 2014, Mojahedin *et al*. 2014, Farzaneh Joubaneh *et al*. 2015, Mojahedin *et al*. 2016, Feyzi and Khorshidvand 2017, Rezaei and Saidi 2017, Barati and Zenkour 2017) or the analysis of the dynamics and the buckling (Chen *et al*. 2017, Kitipornchai *et al*. 2017, Yang *et al*. 2018, Thanh *et al*. 2020) of many porous (imperfect) structures. The most interesting relation to describe the porosity is connected to the tensile moduli (Pabst and Gregorovà 2004a, b, Pabst *et al*. 2004, 2006, Pabst 2014). Akbaş (2017) examined the vibration and bending behavior of FG porous plates. Avcar (2019) investigated the dynamic behavior of imperfect sigmoid and power law functionally graded beams. Abdulrazzaq *et al*. (2020a) presented a numerical formulation for vibration properties of nonlocal porous metal-ceramic plates under periodic dynamic loads. Hadji (2020) discussed the influence of the distribution shape of porosity on the bending response of FG beam using a new HSDT. Gafour *et al*. (2020) studied the porosity-dependent dynamic response of FG nanobeam using "*non-local shear deformation*" and energy principle.

This work is concerned with the influences of humidity and temperature variations on the bending response of AFG porous plates resting on a two-parameter elastic foundation. The differential governing equations for AFG porous plates are determined utilizing the principle of virtual work based on the current model, including hygro-thermal impacts and foundation rigidities. The influences of the porosity parameter, gradient index and other physical and geometrical parameters are all examined. The calculated results are compared with those of other researchers for perfect and imperfect AFG plates.

2. Mathematical model and governing equations

An imperfect AFG plate with a total thickness "h", length "a" and width "b" is considered here (Fig. 1). It is assumed that the material varies only in thickness. The *xy* plane is considered to be the undistorted median plane of the plate and the z axis to be positive upward from the median plane.

Consider a rectangular plate of length a, width b and thickness h made of imperfect functionally graded material. The present problem is studied using an integral plate model for the first time. The applicability and accuracy of the proposed mathematical model for static, buckling and free vibration responses were ascertained in the recent past by several authors. However, the assessment of this model for hygro-thermo-mechanical analysis of the porous AFG ceramic-metal plates is still to be ascertained. In addition, the number of the unknown functions involved in the governing equations is only four.

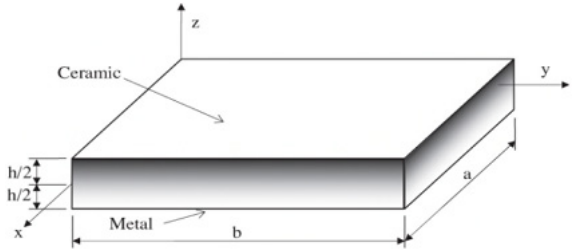

Fig. 1 Geometry of AFG rectangular plate

2.1 Displacement fields and strains

In this article, additional simplifying considerations are made to the traditional HSDT to reduce the number of variables. The displacement field of the traditional HSDT is given by

$$\begin{aligned} u(x,y,z) &= u_0(x,y) - z\frac{\partial w_0}{\partial x} + f(z)\phi_x(x,y) \\ v(x,y,z) &= v_0(x,y) - z\frac{\partial w_0}{\partial y} + f(z)\phi_y(x,y) \\ w(x,y,z) &= w_0(x,y) \end{aligned} \tag{1}$$

where u_0, v_0, w_0, ϕ_x, ϕ_y are "*five unknown displacements*" of the mid-plane of the plate, $f(z)$ presents the shape function which takes into account the variation of the "*transverse shear strains and stresses*" within the thickness. By considering that: $\phi_x = \int \theta(x,y)dx$ and $\phi_y = \int \theta(x,y)dy$, the displacement field of the current theory can be expressed in a simpler form as

$$\begin{aligned} u(x,y,z) &= u_0(x,y) - z\frac{\partial w_0}{\partial x} + k_1 f(z)\int \theta(x,y)\,dx \\ v(x,y,z) &= v_0(x,y) - z\frac{\partial w_0}{\partial y} + k_2 f(z)\int \theta(x,y)\,dy \\ w(x,y,z) &= w_0(x,y) \end{aligned} \tag{2}$$

In this article, the function $f(z)$ is given by

$$f(z) = sin\left(\frac{\pi z}{h}\right) \tag{3}$$

It can be observed that the kinematics in Eq. (2) includes only four variables (u_0, v_0, w_0 and θ).

The constants k_1 and k_2 depend on the geometry.

The nonzero strains associated with the displacement field are

$$\begin{aligned} \begin{Bmatrix} \varepsilon_x \\ \varepsilon_y \\ \gamma_{xy} \end{Bmatrix} &= \begin{Bmatrix} \varepsilon_x^0 \\ \varepsilon_y^0 \\ \gamma_{xy}^0 \end{Bmatrix} + z\begin{Bmatrix} k_x^b \\ k_y^b \\ k_{xy}^b \end{Bmatrix} + f(z)\begin{Bmatrix} k_x^s \\ k_y^s \\ k_{xy}^s \end{Bmatrix}, \\ \begin{Bmatrix} \gamma_{yz} \\ \gamma_{xz} \end{Bmatrix} &= g(z)\begin{Bmatrix} \gamma_{yz}^0 \\ \gamma_{xz}^0 \end{Bmatrix} \end{aligned} \tag{4}$$

where

$$\begin{Bmatrix} \varepsilon_x^0 \\ \varepsilon_y^0 \\ \gamma_{xy}^0 \end{Bmatrix} = \begin{Bmatrix} \dfrac{\partial u_0}{\partial x} \\ \dfrac{\partial v_0}{\partial x} \\ \dfrac{\partial u_0}{\partial y} + \dfrac{\partial v_0}{\partial x} \end{Bmatrix}, \quad \begin{Bmatrix} k_x^b \\ k_y^b \\ k_{xy}^b \end{Bmatrix} = \begin{Bmatrix} -\dfrac{\partial^2 w_0}{\partial x^2} \\ -\dfrac{\partial^2 w_0}{\partial y^2} \\ -2\dfrac{\partial^2 w_0}{\partial x \partial y} \end{Bmatrix}, \tag{5a}$$

$$\begin{Bmatrix} k_x^s \\ k_y^s \\ k_{xy}^s \end{Bmatrix} = \begin{Bmatrix} k_1\theta \\ k_2\theta \\ k_1\dfrac{\partial}{\partial y}\int \theta\, dx + k_2\dfrac{\partial}{\partial x}\int \theta\, dy \end{Bmatrix},$$

$$\begin{Bmatrix}\gamma_{yz}^0\\ \gamma_{xz}^0\end{Bmatrix}=\begin{Bmatrix}k_2\int\theta\,dy\\ k_1\int\theta\,dx\end{Bmatrix}, \tag{5a}$$

and

$$g(z)=\frac{df(z)}{dz} \tag{5b}$$

The analytical solution of this model can be solved by a Navier type solution. The following relations can be determined

$$\begin{aligned}&\frac{\partial}{\partial y}\int\theta\,dx=A'\frac{\partial^2\theta}{\partial x\partial y}, \qquad \frac{\partial}{\partial x}\int\theta\,dy=B'\frac{\partial^2\theta}{\partial x\partial y},\\ &\int\theta\,dx=A'\frac{\partial\theta}{\partial x}, \qquad \int\theta\,dy=B'\frac{\partial\theta}{\partial y}\end{aligned} \tag{6}$$

where the coefficients A', B' (defined according to the type of solution adopted), k_1 and k_2 are expressed as follows

$$A'=-\frac{1}{\lambda^2},\quad B'=-\frac{1}{\mu^2},\quad k_1=\lambda^2,\quad k_2=\mu^2 \tag{7}$$

Note that λ and μ are terms related to the Navier type solution defined in Eq. (17).

2.2 Constitutive equations

The structure is loaded by a sinusoidal distributed pressure $q(x,y)$ and a temperature field $T(x,y,z)$ as well as a moisture concentration $C(x,y,z)$ .The mechanical properties $P(z)$ of the imperfect AFG plate, such as "Young's modulus" E , "Poisson's ratio" ν , "thermal coefficient" α and "moisture expansion" β are provided according to the modified rule of mixture as

$$\begin{aligned}P(z)=P_m+(P_c-P_m)\left(\frac{2z+h}{2h}\right)^k\\ -(P_c+P_m)\left(1-e^{-\zeta/2}\right)\end{aligned} \tag{8}$$

where P_c and P_m are the corresponding mechanical properties of the "*ceramic*" and "*metal*", respectively, and k is the gradient index which takes values greater than or equal to zero, and ζ is the "*porosity volume fraction*" of the imperfect AFG plate ($\zeta << 1$) (Bennai *et al*. 2019). The mechanical properties for the perfect AFG plate can be obtained by setting $\zeta=0$.

The linear constitutive relations are given by

$$\begin{Bmatrix}\sigma_x\\ \sigma_y\\ \tau_{xy}\\ \tau_{yz}\\ \tau_{xz}\end{Bmatrix}=\begin{bmatrix}C_{11}&C_{12}&0&0&0\\ C_{12}&C_{22}&0&0&0\\ 0&0&C_{66}&0&0\\ 0&0&0&C_{44}&0\\ 0&0&0&0&C_{55}\end{bmatrix}\begin{Bmatrix}\varepsilon_x-\alpha\Delta T-\beta\Delta C\\ \varepsilon_y-\alpha\Delta T-\beta\Delta C\\ \gamma_{xy}\\ \gamma_{yz}\\ \gamma_{xz}\end{Bmatrix} \tag{9}$$

where $(\sigma_x,\ \sigma_y,\ \tau_{xy},\ \tau_{yz},\ \tau_{xz})$ and $(\varepsilon_x,\ \varepsilon_y,\ \gamma_{xy},\ \gamma_{yz},\ \gamma_{xz})$ are the stress and strain components, respectively. The stiffness coefficients, C_{ij}, can be given by

$$\begin{aligned}&C_{11}=C_{22}=\frac{E(z)}{1-\nu^2}, \qquad C_{12}=\frac{\nu\,E(z)}{1-\nu^2},\\ &C_{44}=C_{55}=C_{66}=\frac{E(z)}{2(1+\nu)},\end{aligned} \tag{10}$$

where $\Delta T=T-T_0$ and $\Delta C=C-C_0$ in which T_0 is the "*reference temperature*" and C_0 is the "*reference moisture concentration*". The "*temperature and moisture*" field variations within the thickness are supposed to be

$$\Delta T(x,y,z)=T_1(x,y)+\frac{z}{h}T_2(x,y)+\frac{f(z)}{h}T_3(x,y) \tag{11a}$$

$$\Delta C(x,y,z)=C_1(x,y)+\frac{z}{h}C_2(x,y)+\frac{f(z)}{h}C_3(x,y) \tag{11b}$$

2.3 Governing equations

The principle of "*virtual displacements*" is utilized to deduce the equilibrium equations

$$\int_{-h/2}^{h/2}\int_{\Omega}\left[\sigma_x\delta\,\varepsilon_x+\sigma_y\delta\,\varepsilon_y+\tau_{xy}\delta\,\gamma_{xy}+\tau_{xz}\delta\,\gamma_{xz}+\tau_{yz}\delta\,\gamma_{yz}\right]d\,\Omega\,d\,z-\int_{\Omega}(q-f_e)\,\delta\,w\,d\,\Omega=0 \tag{12}$$

Where Ω is the upper face area, and q is the "*applied transverse load*". f_e is the density of the reaction force of foundation. For the "*Pasternak foundation model*" f_e is expressed by

$$f_e=k_w w-k_{p1}\frac{\partial^2 w}{\partial x^2}-k_{p2}\frac{\partial^2 w}{\partial y^2} \tag{13}$$

Where k_w is the modulus of subgrade reaction (Winkler coefficient of the foundation) and k_{p1} and k_{p2} are the shear moduli of the subgrade (shear layer foundation stiffness). If the foundation is "*homogeneous*" and "*isotropic*", we will get $k_{p1}=k_{p2}=k_p$. If the shear layer foundation stiffness is neglected, the "*Pasternak foundation*" becomes a "*Winkler foundation*".

Substituting Eqs. (4) and (9) into Eq. (12), integrating within the thickness of the structure, and setting the coefficients of δu_0, δv_0, δw_0 and $\delta\theta$ to zero separately, the governing equations can be obtained as

$$\begin{aligned}
&\delta u_0: \ \frac{\partial N_x}{\partial x}+\frac{\partial N_{xy}}{\partial y}=0\\
&\delta v_0: \ \frac{\partial N_{xy}}{\partial x}+\frac{\partial N_y}{\partial y}=0\\
&\delta w_0: \ \frac{\partial^2 M_x^b}{\partial x^2}+\frac{\partial^2 M_y^b}{\partial y^2}+2\frac{\partial^2 M_{xy}^b}{\partial x\partial y}+q-f_e=0\\
&\delta\theta: k_1 A' M_x^s+k_2 B' M_y^s+(k_1 (A')^2+k_2(B')^2)\frac{\partial^2 M_{xy}^s}{\partial x\partial y}-k_1(A')^2\frac{\partial Q_{xz}}{\partial x}-k_2(B')^2\frac{\partial Q_{yz}}{\partial y}=0
\end{aligned} \tag{14}$$

Where (N_x, N_y, N_{xy}) denote the total in-plane force resultants, (M_x^b, M_y^b, M_{xy}^b), (M_x^s, M_y^s, M_{xy}^s) are the total moment resultants and (Q_{xz}, Q_{yz}) are the transverse shear stress resultants. They are expressed as

$$\left(N_x, N_y, N_{xy}\right)=\int_{-h/2}^{h/2}\left(\sigma_x,\sigma_y,\tau_{xy}\right)dz \tag{15a}$$

$$\left(M_x^b, M_y^b, M_{xy}^b\right)=\int_{-h/2}^{h/2}\left(\sigma_x,\sigma_y,\tau_{xy}\right)zdz \tag{15b}$$

$$\left(M_x^s, M_y^s, M_{xy}^s\right)=\int_{-h/2}^{h/2}\left(\sigma_x,\sigma_y,\tau_{xy}\right)f(z)dz \tag{15c}$$

$$\begin{aligned}
&\left(Q_{xz}, Q_{yz}\right)=\int_{-\frac{h}{2}}^{\frac{h}{2}}\left(\tau_{xz},\tau_{yz}\right)g(z)dz\\
&\text{with} \quad g(z)=\frac{df}{dz}
\end{aligned} \tag{15d}$$

2.4 Analytical solution

In the present research, the Navier method is utilized to determine the analytical solution for simply supported AFG rectangular plates. The unknown variables are given by

$$\begin{Bmatrix} u_0\\ v_0\\ w_0\\ \theta\end{Bmatrix}=\begin{Bmatrix} U_0\cos(\lambda x)\sin(\mu y)\\ V_0\sin(\lambda x)\cos(\mu y)\\ W_0\sin(\lambda x)\sin(\mu y)\\ \theta_0\sin(\lambda x)\sin(\mu y)\end{Bmatrix} \tag{16}$$

where U_0, V_0, W_0 and θ_0 are arbitrary parameters to be determined, with

$$\lambda=\frac{\pi}{a}, \qquad \mu=\frac{\pi}{b} \tag{17}$$

The following trigonometric form is assumed for the hygro-thermo-mechanical loads (q, T_1, T_2, T_3, C_1, C_2, C_3)

$$\begin{Bmatrix} q\\ T_i\\ C_i\end{Bmatrix}=\begin{Bmatrix} q_0\\ t_i\\ c_i\end{Bmatrix}\sin(\lambda x)\sin(\mu y), \qquad (i=1,2,3) \tag{18}$$

Where q_0, t_i and c_i are the "*Fourier coefficients*" of the hygro-thermo-mechanical loads.

The substitution of Eqs. (16) and (18) into the governing Eq. (14) leads to the following system of algebraic equations

$$[C]\{\Delta\}=\{F\}, \tag{19}$$

Where $\{\Delta\}=\{U_0,V_0,W_0,\theta_0\}^t$ and $[C]$ is the symmetric matrix given by

$$[C]=\begin{bmatrix} S_{11} & S_{12} & S_{13} & S_{14}\\ S_{12} & S_{22} & S_{23} & S_{24}\\ S_{13} & S_{23} & S_{33} & S_{34}\\ S_{14} & S_{24} & S_{34} & S_{44}\end{bmatrix} \tag{20}$$

In which the elements of the stiffness matrix $[C]$ are as follows

$$\begin{aligned}
&S_{11}=\lambda^2A_{11}+\mu^2A_{66}, \quad S_{12}=\lambda\mu(A_{12}+A_{66}),\\
&S_{13}=-(\lambda\mu^2(B_{12}+B_{66})+\lambda^3B_{11}),\\
&S_{14}=\left(\lambda\left(-k_1A'^{\lambda^2D_{11}}-k_2B'^{D_{12}}+\mu^2D_{66}\left(k_1(A')^2+k_2(B')^2\right)\right)\right),\\
&S_{22}=\mu^2A_{22}+\lambda^2A_{66},\\
&S_{23}=-(\lambda^2\mu(B_{12}+2B_{66})+\mu^3B_{22}),\\
&S_{24}=\lambda^2\mu\left(k_1(A')^2+k_2(B')^2\right)D_{66}-\mu(k_1A'^{D_{12}}+k_2B'^{D_{22}}),\\
&S_{33}=-2\lambda^2\mu^2(E_{12}+2E_{66})-\lambda^2\left(k_{p1}+\lambda^2E_{11}\right)-\mu^2\left(k_{p2}+\mu^2E_{22}\right)-k_w,\\
&S_{34}=2\lambda^2\mu^2(k_1(A')^2+k_2(A')^2)F_{66}-\lambda^2(k_1A'^{F_{11}}+k_2B'^{F_{22}})-\mu^2(k_1A'^{F_{12}}+k_2B'^{F_{22}})\\
&S_{44}=-k_1A'^{(k_1A'^{G_{11}}+k_2B'^{G_{12}})}-k_2B'^{(k_1A'^{G_{12}}+k_2B'^{G_{22}})}\\
&\qquad -\lambda^2\mu^2G_{66}\left(k_1(A')^2+k_2(B')^2\right)^2-\lambda^2(k_1^2(A')^3)A_{55}^s-\mu^2(k_2^2(B')^3)A_{44}^s
\end{aligned} \tag{21}$$

And the stiffness components A_{ij}, B_{ij},.., are given as

$$\begin{aligned}
&\left(A_{ij},B_{ij},D_{ij},E_{ij},F_{ij},G_{ij}\right)\\
&=\int_{\frac{-h}{2}}^{\frac{h}{2}}C_{ij}(1,z,f(z),z^2,zf(z),f(z)^2)dz\,,(i,j)\\
&=(1,2,6)
\end{aligned} \tag{22a}$$

$$A_{ij}^{s}=\int_{-\frac{h}{2}}^{\frac{h}{2}} C_{ij}g(z)^2dz\,,(i,j)=(4,5) \tag{22b}$$

And $\{F\}=\{F_1,F_2,F_3,F_4\}^t$ is a generalized force vector given by

$$\begin{aligned}
F_1&=-\lambda\left(\left(A_1^T t_1+\frac{B_1^T}{h}t_2+\frac{B_1^{Ts}}{h}t_3\right)+\left(A_1^c c_1+\frac{B_1^c}{h}c_2+\frac{B_1^{cs}}{h}c_3\right)\right);\\
F_2&=-\mu\left(\left(A_2^T t_1+\frac{B_2^T}{h}t_2+\frac{B_2^{Ts}}{h}t_3\right)+\left(A_2^c c_1+\frac{B_2^c}{h}c_2+\frac{B_2^{cs}}{h}c_3\right)\right)\\
F_3&=-\left(\left(\left(B_1^T(\lambda^2+\mu^2)\right)t_1+\frac{\left(D_1^T(\lambda^2+\mu^2)\right)}{h}t_2+\frac{\left(D_1^{Ts}(\lambda^2+\mu^2)\right)}{h}t_3\right)\right.\\
&\qquad\left.+\left(\left(B_1^c(\lambda^2+\mu^2)\right)c_1+\frac{\left(D_1^c(\lambda^2+\mu^2)\right)}{h}c_2+\frac{\left(D_1^{cs}(\lambda^2+\mu^2)\right)}{h}c_3\right)+q_0\right)\\
F_4&=-\left(B_1^{Ts}(A'k_1+B'k_2)\,t_1+\frac{\left((A'k_1+B'k_2)D_1^{Ts}\right)}{h}\,t_2+\frac{\left((A'k_1+B'k_2)H_1^{Ts}\right)}{h}\,t_3+\left((A'k_1+B'k_2)B_1^{cs}\right)c_1\right.\\
&\qquad\left.+\frac{\left((A'k_1+B'k_2)D_1^{cs}\right)}{h}\,c_2+\frac{\left((A'k_1+B'k_2)H_1^{cs}\right)}{h}\,c_3\right)
\end{aligned} \tag{23}$$

With the stiffness components given as

$$\begin{aligned}
&(A_i^T,B_i^T,D_i^T,B_i^{Ts},D_i^{Ts},H_i^{Ts})\\
&=\int_{\frac{-h}{2}}^{\frac{h}{2}}\alpha(z)C_{ij}(1,z,z^2,f(z),z\,f(z),f(z)^2)dz
\end{aligned} \tag{24a}$$

$$\begin{aligned}
&(A_i^C,B_i^C,D_i^C,B_i^{Cs},D_i^{Cs},H_i^{Cs})\\
&=\int_{\frac{-h}{2}}^{\frac{h}{2}}\beta(z)C_{ij}(1,z,z^2,f(z),z\,f(z),f(z)^2)dz
\end{aligned} \tag{24b}$$

3. Numerical results

To show the effectiveness of the proposed method in predicting the hygro-thermo-mechanical flexure responses of the AFG porous plate, the Titanium/Zerconia of a perfect and an imperfect AFG plate is examined. The used mechanical properties are as follows:

- Titanium (Ti-6Al-4V): $E_m=66.2$GPa, $\nu_m=1/3$, $\alpha_m=10.3$ (10^{-6}/°C), $\beta_m=0.33$
- Zirconia (ZrO_2): $E_c=117.0$ GPa, $\nu_c=1/3$, $\alpha_c=7.11$ (10^{-6}/°C), $\beta_c=0$.

Comparisons are carried out with the different plate models available in the open literature. The reference "*temperature*" and "*moisture*" concentrations are considered with $T_0=25$°C (room temperature) and $C_0=0$%. The non-dimensional parameters employed are

$$\bar{w}=\frac{100D}{q_0a^4}w\left(\frac{a}{2},\frac{b}{2},0\right),\quad \bar{\sigma}_x=\frac{1}{100q_0}\sigma_x\left(\frac{a}{2},\frac{b}{2},\frac{h}{2}\right),$$
$$\bar{\tau}_{xy}=\frac{1}{10q_0}\tau_{xy}\left(0,0,-\frac{h}{3}\right),\quad \bar{\tau}_{xz}=\frac{1}{10q_0}\tau_{xz}\left(0,\frac{b}{2},z\right),$$
$$K_w=\frac{a^4k_w}{D},\quad K_p=\frac{a^2k_p}{D}\quad\text{and}\quad D=\frac{E_ch^3}{12(1-\nu^2)}.$$

The numerical results are presented in Tables 1-4 and graphically in Figs. 2 to 8. It is supposed, unless otherwise stated, that $q_0=100$GPa, $a/h=10$, $b/a=3$, $k=2$, $t_1=t_2=0$, $c_1=c_2=0$.

In Tables 1-3, the computed results are compared with those calculated using the HSDT of Reddy's model (Reddy 2000) and those given by the HSDT of Daouadji *et al*. (2016). These tables also provide the influences of the gradient index and the rigidities of the elastic foundation on the non-dimensional deflection and stresses of the "*perfect and imperfect*" AFG rectangular plate. Table 1 presents the results in the case of mechanical loads. It can be observed that the deflection and stresses decrease with the inclusion of the elastic foundations. The consideration of the Winkler foundation coefficient provides higher values than those with the consideration of the Pasternak foundation coefficients. The deflection increases with increasing the gradient index. The non-dimensional stresses are also sensitive to the gradient index. Tables 2 and 3 present similar results to those provided in Table 1 including the influence of the temperature and humidity fields. In addition, the computed results are compared with those calculated by Reddy's model (Reddy 2000) and the HSDT of Daouadji *et al*. (2016). A very good level of agreement is observed between the proposed theory and the HSDT of Daouadji *et al*. (2016) for all values of the gradient index,

with or without the inclusion of the "*elastic foundation*". It is clear that the stresses for a completely ceramic plate are not the same as for a completely metal plate in the case of the presence of elastic foundations. This is due to the fact that the AFG structure here is affected by the inclusion of the temperature effect. This has a significant impact on the basic structures of the "*rocket launchers*", as a judicious selection of the spatial structure of AFG can effectively extend the life of the structure. Considering the results presented in Tables 1 to 3, it should be noted that the number of unknown variables in the current formulation is four, while the number of these quantities in FSDT and Reddy's theory is five. It can be concluded that the current theory is not only accurate, but also relatively simple. In addition, it is elegant enough to predict the hygro-thermo-mechanical flexure behavior of perfect and imperfect AFG plates resting on elastic foundations. From Tables 1, 2 and 3 it can be concluded that the results of this theory present good agreement with other theories that have a greater number of unknown variables, such as Reddy's theory.

Table 4 shows the influences of the geometric ratio (a/h) and elastic foundation coefficients on the non-dimensional deflection of an imperfect AFG square plate under hygro-thermo-mechanical loads using the current theory. It can be

Table 1 Effect of the gradient index and elastic foundation parameters on the non-dimensional deflection and stresses of AFG rectangular plate with and without porosities ($a/h = 10$, $b = 3a,\ q_0 = 100,\ t_i = c_i = 0$)

k	K_w	K_p	Theory	ζ	$\bar{w}$	$\bar{\sigma}_x$	$\bar{\tau}_{xy}$	$\bar{\tau}_{xz}$
0	0	0	Present	$\zeta = 0$	0.85884	0.51361	0.72790	-0.44295
			Daouadji *et al*. (2016)	$\zeta = 0$	0.85885	0.51364	0.72787	-0.44328
			Reddy's theory	$\zeta = 0$	0.85891	0.51545	0.72797	-0.42956
	100	0	Present	$\zeta = 0$	0.46203	0.27631	0.39157	-0.23831
			Daouadji *et al*. (2016)	$\zeta = 0$	0.46203	0.27632	0.39157	-0.23847
			Reddy's theory	$\zeta = 0$	0.46206	0.27620	0.39162	-0.23109
	0	100	Present	$\zeta = 0$	0.08964	0.053611	0.075971	-0.046236
			Daouadji *et al*. (2016)	$\zeta = 0$	0.08964	0.05361	0.07597	-0.04627
			Reddy's theory	$\zeta = 0$	0.08965	0.05358	0.07599	-0.04485
	100	100	Present	$\zeta = 0$	0.082266	0.049198	0.069722	-0.042431
			Daouadji *et al*. (2016)	$\zeta = 0$	0.08227	0.04920	0.06972	-0.04246
			Reddy's theory	$\zeta = 0$	0.08228	0.04919	0.06972	-0.04116
0.5	100	100	Present	$\zeta = 0$	0.083643	0.046710	0.058125	-0.036065
				$\zeta = 0.1$	0.084279	0.043166	0.053029	-0.032970
				$\zeta = 0.2$	0.084895	0.039743	0.048105	-0.029972
			Daouadji *et al*. (2016)	$\zeta = 0$	0.08364	0.04671	0.05812	-0.03609
				$\zeta = 0.1$	0.08430	0.04308	0.05290	-0.03291
				$\zeta = 0.2$	0.08496	0.03938	0.04758	-0.02968
			Reddy's theory	$\zeta = 0$	0.08366	0.04671	0.05812	-0.03498
2	100	100	Present	$\zeta = 0$	0.084561	0.045411	0.047696	-0.030463
				$\zeta = 0.1$	0.085223	0.041692	0.042382	-0.027231
				$\zeta = 0.2$	0.085868	0.038068	0.037211	-0.024085
			Daouadji *et al*. (2016)	$\zeta = 0$	0.08456	0.04541	0.04769	-0.03049
				$\zeta = 0.1$	0.08523	0.04162	0.04222	-0.02715
				$\zeta = 0.2$	0.08590	0.03768	0.03661	-0.02378
			Reddy's theory	$\zeta = 0$	0.08457	0.04539	0.04770	-0.02951
Metal	100	100	Present	$\zeta = 0$	0.085835	0.029046	0.041160	-0.025050
				$\zeta = 0.1$	0.086072	0.027705	0.039261	-0.023894
				$\zeta = 0.2$	0.086300	0.026424	0.037444	-0.022788
			Daouadji *et al*. (2016)	$\zeta = 0$	0.08584	0.02905	0.04116	-0.02507
				$\zeta = 0.1$	0.08651	0.02522	0.03574	-0.02177
				$\zeta = 0.2$	0.08720	0.02134	0.03024	-0.01842
			Reddy's theory	$\zeta = 0$	0.08584	0.02905	0.04115	-0.02428

Table 2 Effect of the gradient index and elastic foundation parameters on the non-dimensional deflection and stresses of AFG rectangular plate with and without porosities ($a/h = 10$, $b = 3a,\ q_0 = 100,\ t_1 = t_3 = 0,\ t_2 = 10,\ c_1 = c_3 = 0,\ c_2 = 100$)

k	K_w	K_p	Theory	ζ	$\bar{w}$	$\bar{\sigma}_x$	$\bar{\tau}_{xy}$	$\bar{\tau}_{xz}$
Ceramic	0	0	Present	$\zeta = 0$	1.8070	0.47200	1.5597	-0.44295
			Daouadji *et al*. (2016)	$\zeta = 0$	1.80707	0.47204	1.55974	-0.44328
			Reddy's theory	$\zeta = 0$	1.80712	0.47187	1.55982	-0.42955
	100	0	Present	$\zeta = 0$	0.97214	-0.027290	0.85215	-0.012340
			Daouadji *et al*. (2016)	$\zeta = 0$	0.97214	-0.02729	0.85215	-0.01235
			Reddy's theory	$\zeta = 0$	0.97216	-0.02740	0.85211	-0.01197
	0	100	Present	$\zeta = 0$	0.18861	-0.49589	0.18808	0.39180
			Daouadji *et al*. (2016)	$\zeta = 0$	0.18861	-0.49588	0.18810	0.39206
			Reddy's theory	$\zeta = 0$	0.18861	-0.49570	0.18806	0.37990
	100	100	Present	$\zeta = 0$	0.17310	-0.50516	0.17494	0.39980
			Daouadji *et al*. (2016)	$\zeta = 0$	0.17309	-0.50516	0.17495	0.40007
			Reddy's theory	$\zeta = 0$	0.17309	-0.50498	0.17490	0.38766
0.5	100	100	Present	$\zeta = 0$	0.18411	-0.52001	0.18300	0.45696
				$\zeta = 0.1$	0.16593	-0.42416	0.15218	0.36813
				$\zeta = 0.2$	0.15027	-0.34102	0.12653	0.29159
			Daouadji *et al*. (2016)	$\zeta = 0$	0.18411	-0.51999	0.18301	0.45727
				$\zeta = 0.1$	0.16549	-0.42187	0.15147	0.36625
				$\zeta = 0.2$	0.14872	-0.33279	0.12405	0.28426
			Reddy's theory	$\zeta = 0$	0.18410	-0.51975	0.18299	0.44334
1	100	100	Present	$\zeta = 0$	0.18504	-0.51478	0.15635	0.45954
				$\zeta = 0.1$	0.16666	-0.41882	0.12647	0.37005
				$\zeta = 0.2$	0.15081	-0.33554	0.10164	0.29289
			Daouadji *et al*. (2016)	$\zeta = 0$	0.18504	-0.51475	0.15636	0.45986
				$\zeta = 0.1$	0.16621	-0.41652	0.12578	0.36814
				$\zeta = 0.2$	0.14925	-0.32731	0.09924	0.28549
			Reddy's theory	$\zeta = 0$	0.18504	-0.51450	0.15631	0.44545
2	100	100	Present	$\zeta = 0$	0.18559	-0.50365	0.13459	0.45304
				$\zeta = 0.1$	0.16704	-0.40772	0.10567	0.36357
				$\zeta = 0.2$	0.15103	-0.32443	0.081742	0.28646
			Daouadji *et al*. (2016)	$\zeta = 0$	0.18559	-0.50363	0.13461	0.45337
				$\zeta = 0.1$	0.16659	-0.40543	0.10501	0.36169
				$\zeta = 0.2$	0.14945	-0.31618	0.079451	0.27908
			Reddy's theory	$\zeta = 0$	0.18560	-0.50336	0.13451	0.43831
metal	100	100	Present	$\zeta = 0$	0.18840	-0.43118	0.12090	0.47432
			Daouadji *et al*. (2016)	$\zeta = 0$	0.18840	-0.43117	0.12092	0.47465
			Reddy's theory	$\zeta = 0$	0.18840	-0.43095	0.12087	0.45993

observed from this Table (and also Fig. 2) that the deflection diminishes as the geometric ratio *a*/*h* increases. This because of the considerable impact of temperature and humidity on the "*extensional behavior*" of the AFG plate compared to the "*flexural behavior*". In addition, the inclusion of elastic foundations leads to a reduction of the values of the deflections.

Figs. 2(a) and (b) present the variations of the "center deflection" vs. the geometric ratio (*b*/*a*) for different types of AFG porous plates. It can be seen that the deflection decreases in the presence of the foundations, while the influence of the humidity parameter turns out to be lower than that of the temperature. From Fig. 2(a) it can be observed that the transversal displacement (deflection) takes the greater value for the metallic plate and the lower one for

Table 3 Effect of the gradient index and elastic foundation parameters on the non-dimensional deflection and stresses of AFG rectangular plate with and without porosities ($a/h = 10$, $b = 3a,\ q_0 = 100,\ t_1 = 0,\ t_2 = t_3 = 10,\ c_1 = 0,\ c_2 = c_3 = 100$)

k	K_w	K_p	Theory	ζ	$\bar{w}$	$\bar{\sigma}_x$	$\bar{\tau}_{xy}$	$\bar{\tau}_{xz}$
Ceramic	0	0	Present	$\zeta = 0$	2.5407	0.52552	2.2037	-0.43724
			Daouadji *et al*. (2016)	$\zeta = 0$	2.54067	0.52554	2.20366	-0.43753
			Reddy's theory	$\zeta = 0$	2.54076	0.52522	2.20374	-0.42454
	100	0	Present	$\zeta = 0$	1.3668	-0.17651	1.2089	0.16822
			Daouadji *et al*. (2016)	$\zeta = 0$	1.36680	-0.17649	1.20881	0.16834
			Reddy's theory	$\zeta = 0$	1.36682	-0.17643	1.20877	0.16257
	0	100	Present	$\zeta = 0$	0.26517	-0.83532	0.27515	0.73642
			Daouadji *et al*. (2016)	$\zeta = 0$	0.26517	-0.83532	0.27518	0.73692
			Reddy's theory	$\zeta = 0$	0.26518	-0.83500	0.27507	0.71354
	100	100	Present	$\zeta = 0$	0.24335	-0.84838	0.25666	0.74769
			Daouadji *et al*. (2016)	$\zeta = 0$	0.24336	-0.84837	0.25669	0.74817
			Reddy's theory	$\zeta = 0$	0.24336	-0.84804	0.25658	0.72442
0.5	100	100	Present	$\zeta = 0$	0.26196	-0.87285	0.28039	0.84531
				$\zeta = 0.1$	0.22923	-0.71615	0.22961	0.68416
				$\zeta = 0.2$	0.20098	-0.57978	0.18784	0.54506
			Daouadji *et al*. (2016)	$\zeta = 0$	0.26196	-0.87282	0.28041	0.84587
				$\zeta = 0.1$	0.22844	-0.71238	0.22844	0.68075
				$\zeta = 0.2$	0.19820	-0.56627	0.18386	0.53174
			Reddy's theory	$\zeta = 0$	0.26195	-0.87239	0.28034	0.81947
1	100	100	Present	$\zeta = 0$	0.26330	-0.86255	0.23769	0.84806
				$\zeta = 0.1$	0.23019	-0.70559	0.18868	0.68566
				$\zeta = 0.2$	0.20160	-0.56894	0.14849	0.54539
			Daouadji *et al*. (2016)	$\zeta = 0$	0.26330	-0.86250	0.23772	0.84866
				$\zeta = 0.1$	0.22940	-0.70179	0.18756	0.68224
				$\zeta = 0.2$	0.19878	-0.55537	0.14466	0.53196
			Reddy's theory	$\zeta = 0$	0.26330	-0.86205	0.23762	0.82148
2	100	100	Present	$\zeta = 0$	0.26394	-0.84187	0.20151	0.83421
				$\zeta = 0.1$	0.23053	-0.68489	0.15426	0.67176
				$\zeta = 0.2$	0.20164	-0.54808	0.11578	0.53149
			Daouadji *et al*. (2016)	$\zeta = 0$	0.26394	-0.84183	0.20154	0.83481
				$\zeta = 0.1$	0.22972	-0.68110	0.15319	0.66835
				$\zeta = 0.2$	0.19878	-0.53449	0.11213	0.51806
			Reddy's theory	$\zeta = 0$	0.26396	-0.84138	0.20133	0.80652
5	100	100	Present	$\zeta = 0$	0.26599	-0.81794	0.18483	0.83169
				$\zeta = 0.1$	0.23230	-0.66194	0.66194	0.66826
				$\zeta = 0.2$	0.20313	-0.52579	0.10158	0.52721
			Daouadji *et al*. (2016)	$\zeta = 0$	0.26599	-0.81790	0.18486	0.83228
				$\zeta = 0.1$	0.23148	-0.65816	0.13785	0.66489
				$\zeta = 0.2$	0.20025	-0.51226	0.09805	0.51369
			Reddy's theory	$\zeta = 0$	0.26601	-0.81745	0.18459	0.80297
Metal	100	100	Present	$\zeta = 0$	0.26776	-0.71696	0.18297	0.86686
			Daouadji *et al*. (2016)	$\zeta = 0$	0.26775	-0.71694	0.18299	0.86749
			Reddy's theory	$\zeta = 0$	0.26774	-0.71656	0.18286	0.84003

Table 4 Effects of side-to-thickness ratio and elastic foundation parameters on non-dimensional deflection of an AFG square plate ($q_0 = 100,\ t_1 = 0,\ t_2 = t_3 = 10,\ c_1 = 0,\ c_2 = c_3 = 100$)

k	K_w	K_p	ζ	a/h				
				5	10	20	50	100
0.5	0	0	$\zeta = 0$	5.2887	1.5561	0.62188	0.36020	0.32281
			$\zeta = 0.1$	4.7875	1.4549	0.62062	0.38696	0.35358
			$\zeta = 0.2$	4.3168	1.3653	0.62634	0.41937	0.38981
	100	0	$\zeta = 0$	3.8334	1.1719	0.47300	0.27475	0.24633
			$\zeta = 0.1$	3.3752	1.0684	0.46065	0.28808	0.26334
			$\zeta = 0.2$	2.9495	0.97439	0.45215	0.30372	0.28244
	0	100	$\zeta = 0$	0.62274	0.20826	0.086214	0.050449	0.045278
			$\zeta = 0.1$	0.51704	0.17874	0.079009	0.049770	0.045544
			$\zeta = 0.2$	0.42522	0.15309	0.072791	0.049240	0.045839
	100	100	$\zeta = 0$	0.59610	0.19951	0.082615	0.048341	0.043389
			$\zeta = 0.1$	0.49470	0.17114	0.075671	0.047666	0.043619
			$\zeta = 0.2$	0.40663	0.14650	0.069672	0.047134	0.043876
2	0	0	$\zeta = 0$	6.0767	1.7913	0.71640	0.41516	0.37211
			$\zeta = 0.1$	5.5848	1.7017	0.72716	0.45409	0.41506
			$\zeta = 0.2$	5.1278	1.6281	0.74944	0.50318	0.46799
	100	0	$\zeta = 0$	4.2097	1.2986	0.52552	0.30556	0.27402
			$\zeta = 0.1$	3.7274	1.1930	0.51640	0.32366	0.29599
			$\zeta = 0.2$	3.2759	1.0971	0.51220	0.34526	0.32131
	0	100	$\zeta = 0$	0.62299	0.21097	0.087688	0.051386	0.046131
			$\zeta = 0.1$	0.51537	0.18068	0.080284	0.050704	0.046422
			$\zeta = 0.2$	0.42173	0.15429	0.073888	0.050177	0.046745
	100	100	$\zeta = 0$	0.59589	0.20196	0.083959	0.049201	0.044171
			$\zeta = 0.1$	0.49272	0.17286	0.076822	0.048520	0.044424
			$\zeta = 0.2$	0.40298	0.14752	0.070659	0.047989	0.044707
10	0	0	$\zeta = 0$	6.8157	2.0078	0.80051	0.46209	0.41374
			$\zeta = 0.1$	6.3364	1.9285	0.82115	0.51074	0.46637
			$\zeta = 0.2$	5.8963	1.8690	0.85673	0.57287	0.53232
	100	0	$\zeta = 0$	4.5465	1.4106	0.57015	0.33038	0.29598
			$\zeta = 0.1$	4.0402	1.3020	0.56283	0.35156	0.32122
			$\zeta = 0.2$	3.5628	1.2032	0.56087	0.37683	0.35041
	0	100	$\zeta = 0$	0.62803	0.21458	0.089183	0.052102	0.046731
			$\zeta = 0.1$	0.51860	0.18369	0.081621	0.051395	0.047014
			$\zeta = 0.2$	0.42332	0.15676	0.075074	0.050841	0.047328
	100	100	$\zeta = 0$	0.60042	0.20529	0.085344	0.049861	0.044721
			$\zeta = 0.1$	0.49554	0.17563	0.078063	0.049156	0.044967
			$\zeta = 0.2$	0.40430	0.14981	0.071756	0.048598	0.045240

the ceramic plate and this for all values of temperature, moisture, and elastic foundation rigidities. All structures with intermediate characteristics undergo corresponding "intermediate values" of transversal displacement. From Fig. 2(b), it can be seen that the porosity increases the deflection.

Fig. 3 illustrates the variation of the transversal displacement with the temperature load parameter (t_2) for perfect and imperfect AFG plates resting on an elastic foundation. It can be shown that the deflection varies linearly with t_2 and that the influence of the porosity parameter becomes more important for high values of the temperature load parameter (t_2).

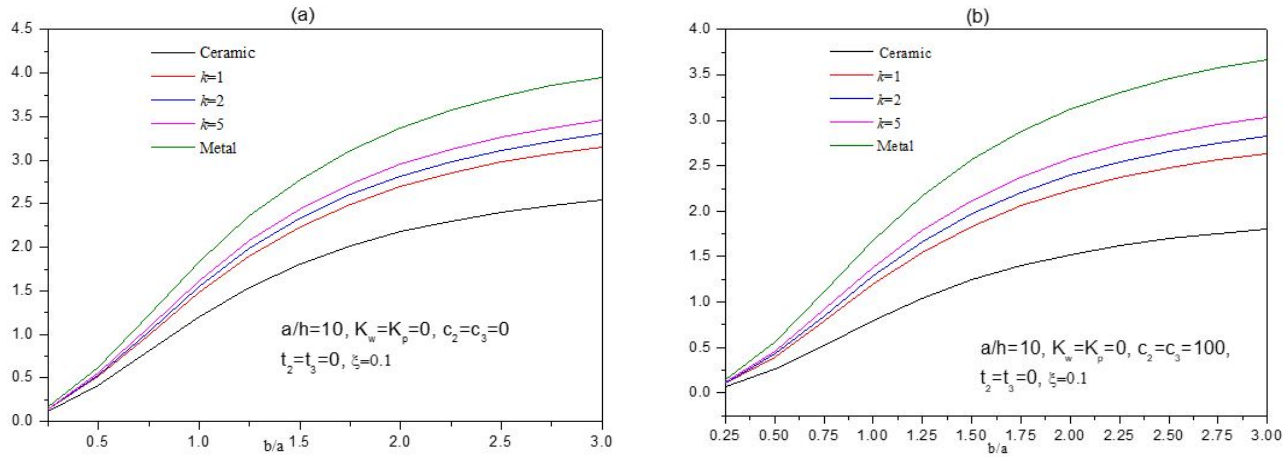

(a) (b)

Fig. 2 (a) Non-dimensional deflection $\bar{w}$ versus the geometric ratio b/a for imperfect AFG plate

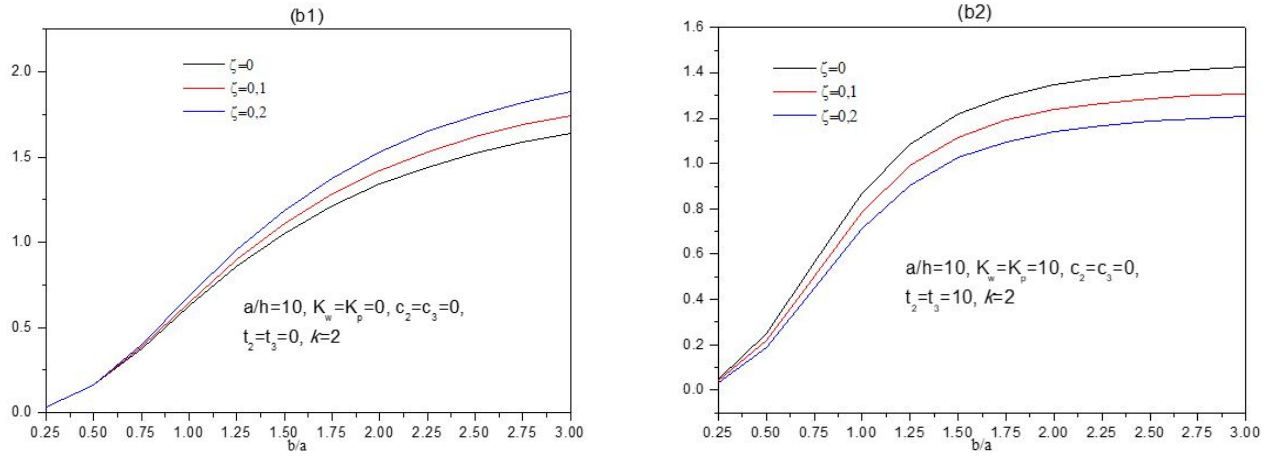

(a) (b)

Fig. 2 (b) Effect of porosity on the variation non-dimensional deflection $\bar{w}$ with the geometric ratio b/a of AFG plate

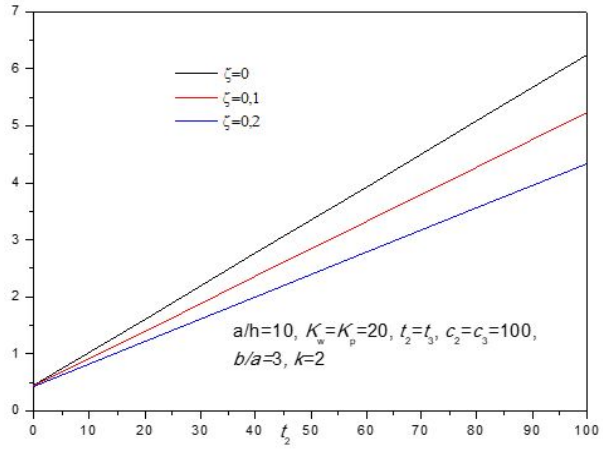

Fig. 3 Non-dimensional center deflection $\bar{w}$ of imperfect and perfect AFG plates on elastic foundations versus t_2 for different values of the porosity parameter

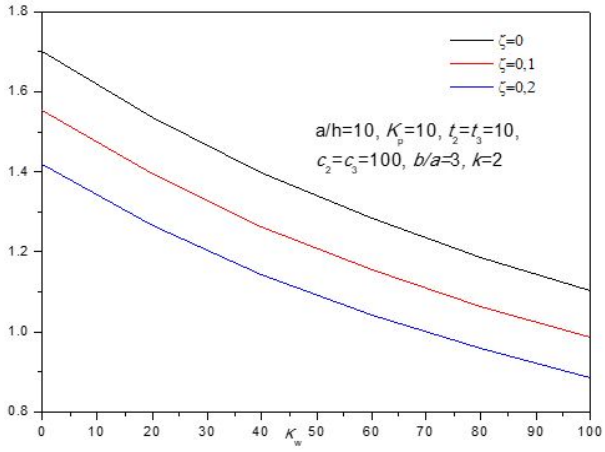

Fig. 4 Effect of the Winkler parameter K_w on Non-dimensional center deflection $\bar{w}$ of imperfect and perfect AFG plates

Fig. 4 demonstrates the impact of the Winkler coefficient K_w on a non-dimensional deflection of perfect and imperfect AFG plates. We see that the Winkler coefficient and the porosity parameter simultaneously reduce the values of the deflections.

Similarly, Fig. 5 shows the influence of the Pasternak

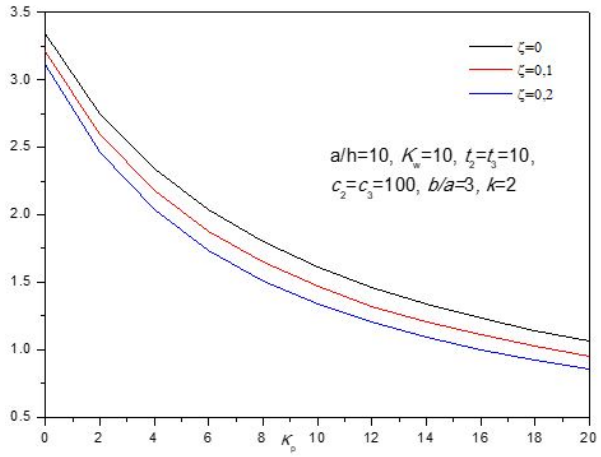

Fig. 5 Effect of the Pasternak parameter K_p on Non-dimensional center deflection $\bar{w}$ of imperfect and perfect AFG plates

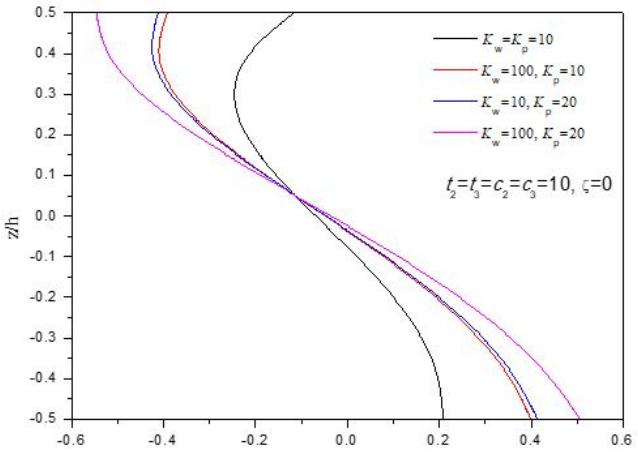

Fig. 7 Effect of the elastic foundation parameters on the variation of $\bar{\sigma}_x$ across the thickness of perfect AFG plates

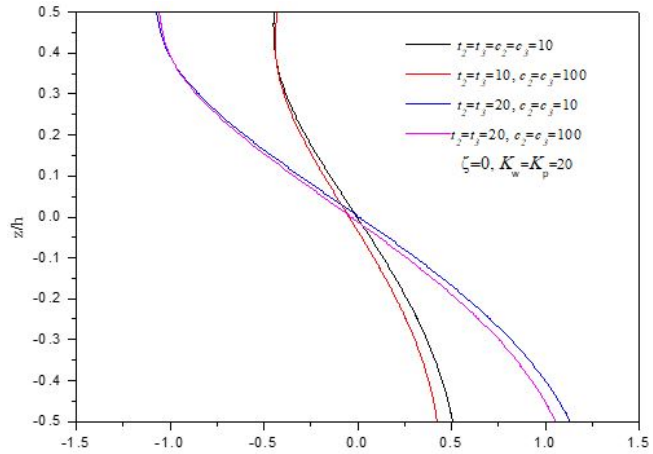

Fig. 6 (a) Effect of humidity and temperature fields on the variation of $\bar{\sigma}_x$ across the thickness of perfect AFG plates resting on elastic foundation

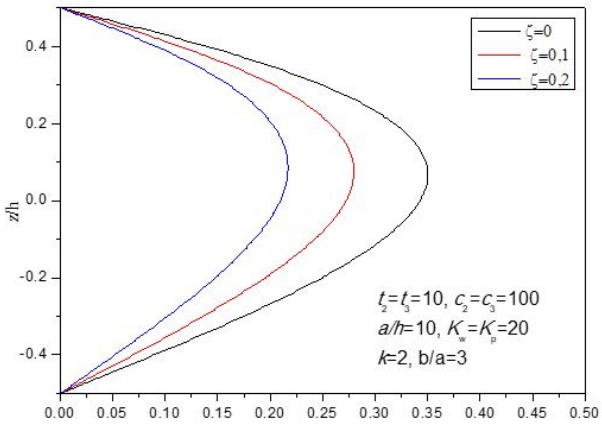

Fig. 8 Effect of the porosity on the variation of $\bar{\tau}_{xz}$ across the thickness of AFG plates resting on elastic foundation

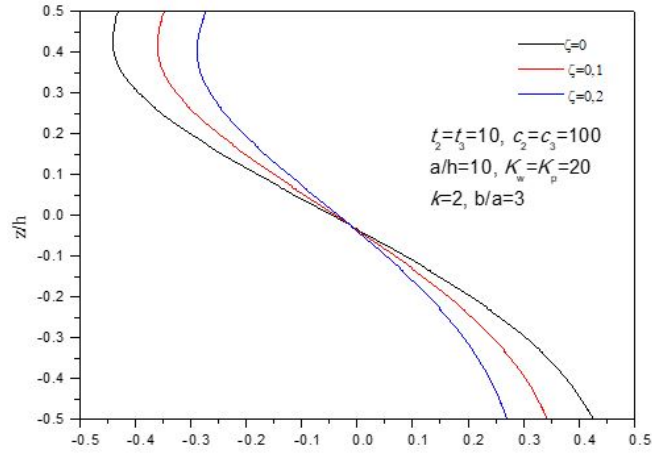

Fig. 6 (b) Effect of the porosity on the variation of $\bar{\sigma}_x$ across the thickness of AFG plates resting on elastic foundation

coefficient K_p on the non-dimensional deflection of perfect and imperfect AFG plates.

Figs. 6 and 7 present the variations of the non-dimensional axial stress ($\bar{\sigma}_x$) across the thickness of the imperfect AFG rectangular plates. The influence of the humidity and temperature fields on $\bar{\sigma}_x$ is demonstrated in Fig. 6(a), and the effect of porosity is shown in Fig. 6(b), while the influence of the "*elastic foundations*" parameters is presented in Fig. 7. It can be shown from Fig. 6 that the upper face is in a maximum compressive state, while the lower one is in a maximum tensile state. It is also clear that the effect of porosity is more pronounced in the upper and lower faces. As shown in Fig. 7 the elastic foundation has an important impact on the maximum values of the "*non-dimensional axial stress*".

Fig. 8 illustrates the influence of porosity on the non-dimensional stress $\bar{\tau}_{xz}$ of AFG plates. It is also clear that the effect of porosity is more pronounced in the center face.

4. Conclusions

In this article, the hygro-thermo-mechanical bending response of perfect and imperfect AFG ceramic-metal plates resting on elastic foundations is studied by using an integral plate model. Because of the presence of porosity, a modified rule of mixture is considered to predict the mechanical properties of the AFG plates. The influences of the porosity and other physical and geometrical parameters on the hygro-thermo-mechanical bending response of AFG plates are investigated. In obtaining from numerical results, the porosity changes the hygro-thermo-mechanical bending behavior of AFG ceramic-metal plates, significantly. The porosity distribution, the gradient index and the rigidities of the elastic foundation have a great influence on the hygro-thermo-mechanical bending behavior of AFG plates. Other types of materials can be also considered in the future (Yeghnem *et al*. 2017, Panjehpour *et al*. 2018, Shahadat *et al*. 2018, Selmi and Bisharat 2018, Natanzi *et al*. 2018, Rajabi and Mohammadimehr 2019, Fadoun 2019, Ghannadpour and Mehrparvar 2020, Selmi 2020, Kertész *et al*.2020, Saini and Lal 2020, Tayeb et al. 2020, Sahoo *et al*. 2020, Arefi and Żur 2020, Mahmoud *et al*. 2020, Yaghoobi and Taheri 2020, Timesli 2020, Akbaş *et al*. 2020, Ashraf *et al*. 2020, Abdulrazzaq *et al*. 2020b).

Acknowledgments

The authors would like to acknowledge the support provided by the Deanship of Scientific Research (DSR) at King Fahd University of Petroleum & Minerals (KFUPM), Saudi Arabia for funding this work through Project No. DF181032. The support provided by the Department of Civil and Environmental Engineering is also acknowledged.

References

Abdalla, J.A. and Ibrahim, A.M. (2006), "Development of a discrete Reissner-Mindlin element on Winkler foundation", *Finite Elem. Anal. Des.*, **42**, 740-748. https://doi.org/10.1016/j.finel.2005.11.004

Abdulrazzaq, M.A. Kadhim, Z.D., Faleh, N.M. and Moustafa, N.M. (2020a), "A numerical method for dynamic characteristics of nonlocal porous metal-ceramic plates under periodic dynamic loads", *Struct. Monitor. Maint., Int. J.*, **7**(1), 27-42. https://doi.org/10.12989/smm.2020.7.1.027

Abdulrazzaq, M.A., Fenjan, R.M., Ahmed, R.A. and Faleh, N.M. (2020b), "Thermal buckling of nonlocal clamped exponentially graded plate according to a secant function based refined theory", *Steel Compos. Struct., Int. J.*, **35**(1), 147-157. https://doi.org/10.12989/scs.2020.35.1.147

Akbaş, Ş.D. (2017), "Vibration and static analysis of functionally graded porous plates", *J. Appl. Computat. Mech.*, **3**(3), 199-207. https://doi.org/10.22055/JACM.2017.21540.1107

Akbaş, Ş.D., Fageehi, Y.A., Assie, A.E. and Eltaher, M.A. (2020), "Dynamic analysis of viscoelastic functionally graded porous thick beams under pulse load", *Eng. Comput.* https://doi.org/10.1007/s00366-020-01070-3

Arefi, M. and Żur, K.K. (2020), "Free vibration analysis of functionally graded cylindrical nanoshells resting on Pasternak foundation based on two-dimensional analysis", *Steel Compos. Struct., Int. J.*, **34**(4), 615-623. http://dx.doi.org/10.12989/scs.2020.34.4.615

Ashraf, M.A., Liu, Z., Zhang, D. and Pham, B.T. (2020), "Effects of elastic foundation on the large-amplitude vibration analysis of functionally graded GPL-RC annular sector plates", *Eng. Comput.* https://doi.org/10.1007/s00366-020-01068-x

Attia, M.A. (2017), "On the mechanics of functionally graded nanobeams with the account of surface elasticity", *Int. J.of Eng. Sci.*, **115**, 73-101. https://doi.org/10.1016/j.ijengsci.2017.03.011

Avcar, M. (2019), "Free vibration of imperfect sigmoid and power law functionally graded beams", *Steel Compos. Struct., Int. J.*, **30**(6), 603-615. https://doi.org/10.12989/SCS.2019.30.6.603

Avcar, M. and Mohammed, W.K.M. (2018), "Free vibration of functionally graded beams resting on Winkler-Pasternak foundation", *Arab. J. Geosci.*, **11**(10), 232. https://doi.org/10.1007/s12517-018-3579-2

Barati, M.R. and Zenkour, A.M. (2017), "Investigating post-buckling of geometrically imperfect metal foam nanobeams with symmetric and asymmetric porosity distributions", *Compos. Struct.*, **182**, 91-98. https://doi.org/10.1016/j.compstruct.2017.09.008

Behravan Rad, A. and Shariyat, M. (2015), "Three-dimensional magneto-elastic analysis of asymmetric variable thickness porous FGM circular plates with non-uniform tractions and Kerr elastic foundations", *Compos. Struct.*, **125**, 558-574. https://doi.org/10.1016/j.compstruct.2015.02.049

Bennai, R., Fourn, H., Ait Atmane, H., Tounsi, A. and Bessaim, A. (2019), "Dynamic and wave propagation investigation of FGM plates with porosities using a four variable plate theory", *Wind Struct., Int. J.*, **28**(1), 49-62. http://dx.doi.org/10.12989/was.2019.28.1.049

Birman, V. and Byrd, L.W. (2007), "Modeling and analysis of functionally graded materials and structures", *Appl. Mech. Rev.*, **60**, 195-216. https://doi.org/10.1115/1.2777164

Boulal, A., Bensattalah, T., Karas, A., Zidour, M., Heireche, H. and Adda Bedia, E.A. (2020), "Buckling of carbon nanotube reinforced composite plates supported by Kerr foundation using Hamilton's energy principle", *Struct. Eng. Mech., Int. J.*, **73**(2), 209-223. https://doi.org/10.12989/sem.2020.73.2.209

Carrera, E., Brischetto, S. and Robaldo, A. (2008), "Variable kinematic model for the analysis of functionally graded material plates", *AIAA J.*, **46**, 194-203. https://doi.org/10.2514/1.32490

Carrera, E., Brischetto, S., Cinefra, M. and Soave, M. (2011), "Effects of thickness stretching in functionally graded plates and shells", *Compos. Part B*, **42**, 123-133. https://doi.org/10.1016/j.compositesb.2010.10.005

Chen, D., Kitipornchai, S. and Yang, J. (2016), "Nonlinear free vibration of shear deformable sandwich beam with a functionally graded porous core", *Thin-Wall. Struct.*, **107**, 39-48. https://doi.org/10.1016/j.tws.2016.05.025

Chen, D., Yang, J. and Kitipornchai, S. (2017), "Nonlinear vibration and postbuckling of functionally graded graphene reinforced porous nanocomposite beams", *Compos. Sci. Technol.*, **142**, 235-245. https://doi.org/10.1016/j.compscitech.2017.02.008

Chucheepsakul, S. and Chinnaboon, B. (2002), "An alternative domain/boundary element technique for analyzing plates on two-parameter elastic foundations", *Eng. Anal. Bound. Elem.*, **26**, 547-555. https://doi.org/10.1016/S0955-7997(02)00007-3

Civalek, O. (2007a), "Nonlinear analysis of thin rectangular plates on Winkler-Pasternak elastic foundations by DSCHDQ methods", *Appl. Math. Model.*, **31**, 606-624. https://doi.org/10.1016/j.apm.2005.11.023

Civalek, O. (2007b), "Three-dimensional vibration, buckling and bending analyses of thick rectangular plates based on discrete singular convolution method", *Int. J. Mech. Sci.*, **49**, 752-765.

https://doi.org/10.1016/j.ijmecsci.2006.10.002
Daouadji, T.H., Adim, B. and Benferhat, R. (2016), "Bending analysis of an imperfect FGM plates under hygro-thermo-mechanical loading with analytical validation", *Adv. Mater. Res., Int. J.*, **5**(1), 35-53. http://dx.doi.org/10.12989/amr.2016.5.1.035
Dehshahri, K., Nejad, M.Z., Ziaee, S., Niknejad, A. and Hadi, A. (2020), "Free vibrations analysis of arbitrary three-dimensionally FGM nanoplates", *Adv. Nano Res., Int. J.*, **8**(2), 115-134. http://dx.doi.org/10.12989/anr.2020.8.2.115
Duc, N.D. and Tung, H.V. (2011), "Mechanical and thermal postbuckling of higher order shear deformable functionally graded plates on elastic foundations", *Compos. Struct.*, **93**, 2874-2881. https://doi.org/10.1016/j.compstruct.2011.05.017
Fadoun, O.O. (2019), "Analysis of axisymmetric fractional vibration of an isotropic thin disc in finite deformation", *Comput. Concrete, Int. J.*, **23**(5), 303-309. http://dx.doi.org/10.12989/cac.2019.23.5.303
Faleh, N.M., Ahmed, R.A. and Fenjan, R.M. (2018), "On vibrations of porous FG nanoshells", *Int. J. Eng. Sci.*, **133**, 1-14. https://doi.org/10.1016/j.ijengsci.2018.08.007
Farzaneh Joubaneh, E., Mojahedin, A., Khorshidvand, A.R. and Jabbari, M. (2015), "Thermal buckling analysis of porous circular plate with piezoelectric sensor-actuator layers under uniform thermal load", *J. Sandw. Struct. Mater.*, **17**, 3-25. https://doi.org/10.1177/1099636214554172
Fenjan, N.M., Moustafa, N.M. and Faleh, N.M. (2020), "Scale-dependent thermal vibration analysis of FG beams having porosities based on DQM", *Adv. Nano Res., Int. J.*, **8**(4), 283-292. https://doi.org/10.12989/anr.2020.8.4.283
Fesharaki, J.J. and Roghani, M. (2019), "Elastic behavior of functionally graded two tangled circles chamber", *J. Appl. Computat. Mech.*, **5**(4), 667-679. https://doi.org/10.22055/JACM.2019.27058.1372
Feyzi, M.R. and Khorshidvand, A.R. (2017), "Axisymmetric post-buckling behavior of saturated porous circular plates", *Thin-Wall. Struct.*, **112**, 149-158. https://doi.org/10.1016/j.tws.2016.11.026
Gafour, Y., Hamidi, A., Benahmed, A., Zidour, M. and Bensattalah, T. (2020), Porosity-dependent free vibration analysis of FG nanobeam using non-local shear deformation and energy principle", *Adv. Nano Res., Int. J.*, **8**(1), 37-47. https://doi.org/10.12989/anr.2020.8.1.037
Ghannadpour, S.A.M. and Mehrparvar, M. (2020), "Nonlinear and post-buckling responses of FGM plates with oblique elliptical cutouts using plate assembly technique", *Steel Compos. Struct., Int. J.*, **34**(2), 227-239. http://dx.doi.org/10.12989/scs.2020.34.2.227
Hadji, L. (2020), "Influence of the distribution shape of porosity on the bending of FGM beam using a new higher order shear deformation model", *Smart Struct. Syst., Int. J.*, **26**(2), 253-262. https://doi.org/10.12989/sss.2020.26.2.253
Han, J.B. and Liew, K.M. (1997), "Numerical differential quadrature method for Reissner /Mindlin plates on two-parameter foundations", *Int. J. Mech. Sci.*, **39**, 977-989. https://doi.org/10.1016/S0020-7403(97)00001-5
Heidari, F., Afsari, A. and Janghorban, M. (2020), "Several models for bending and buckling behaviors of FG-CNTRCs with piezoelectric layers including size effects", *Adv. Nano Res., Int. J.*, **9**(3), 193-210. http://doi.org/10.12989/anr.2020.9.3.193
Jena, S.K., Chakraverty, S. and Malikan, M. (2020), "Application of shifted Chebyshev polynomial-based Rayleigh–Ritz method and Navier's technique for vibration analysis of a functionally graded porous beam embedded in Kerr foundation", *Eng. Comput.* https://doi.org/10.1007/s00366-020-01018-7
Kasaeian, A.B., Vatan, SH.N. and Daneshmand, S. (2011), "FGM materials and finding an appropriate model for the thermal conductivity", *Procedia Eng.*, **14**, 3199-3204. https://doi.org/10.1016/j.proeng.2011.07.404
Kertész, S., Szerencsés, S.G., Veréb, G., Csanádi, J., László, Z. and Hodúr, C. (2020), "Single- and multi-stage dairy wastewater treatment by vibratory membrane separation processes", *Membr. Water Treat., Int. J.*, **11**(6), 383-389. http://doi.org/10.12989/mwt.2020.11.6.383
Khorshidvand, A.R., Farzaneh Joubaneh, E., Jabbari, M. and Eslami, M.R. (2014), "Buckling analysis of a porous circular plate with piezoelectric sensoractuator layers under uniform radial compression", *Acta Mech.*, **225**, 179-193. https://doi.org/10.1007/s00707-013-0959-2
Kitipornchai, S., Chen, D. and Yang, J. (2017), "Free vibration and elastic buckling of functionally graded porous beams reinforced by graphene platelets", *Mater. Des.*, **116**, 656-665. https://doi.org/10.1016/j.matdes.2016.12.061
Madenci, E. (2019), "A refined functional and mixed formulation to static analyses of fgm beams", *Struct. Eng. Mech., Int. J.*, **69**(4), 427-437. https://doi.org/10.12989/sem.2019.69.4.427
Mahmoud, S.R., Al-Solami, H.M., Alkenani, N., Alhebshi, A.M.S., Alwabli, A.S. and Bahieldin, A. (2020), "A mechanical model to investigate Aedesaegypti mosquito bite using new techniques and its applications", *Membr. Water Treat., Int. J.*, **11**(6), 399-406. http://doi.org/10.12989/mwt.2020.11.6.399
Mehar, K. and Panda, S.K. (2017a), "Numerical investigation of nonlinear thermomechanical deflection of functionally graded CNT reinforced doubly curved composite shell panel under different mechanical loads", *Compos. Struct.*, **161**, 287-298. https://doi.org/10.1016/j.compstruct.2016.10.135
Mehar, K. and Panda, S.K. (2017b), "Thermoelastic analysis of FG-CNT reinforced shear deformable composite plate under various loadings", *Int. J. Comput. Meth.*, **14**(2), 1750019. https://doi.org/10.1142/S0219876217500190
Mojahedin, A., Farzaneh Joubaneh, E. and Jabbari, M. (2014), "Thermal and mechanical stability of a circular porous plate with piezoelectric actuators", *Acta Mech.*, **225**, 3437-3452. https://doi.org/10.1007/s00707-014-1153-x
Mojahedin, A., Jabbari, M., Khorshidvand, A.R. and Eslami, M.R. (2016), "Buckling analysis of functionally graded circular plates made of saturated porous materials based on higher order shear deformation theory", *Thin-Wall. Struct.*, **99**, 83-90. https://doi.org/10.1016/j.tws.2015.11.008
Natanzi, A.J., Jafari, G.S. and Kolahchi, R. (2018), "Vibration and instability of nanocomposite pipes conveying fluid mixed by nanoparticles resting on viscoelastic foundation", *Comput. Concrete, Int. J.*, **21**(5), 569-582. http://doi.org/10.12989/cac.2018.21.5.569
Ozgan, K. and Daloglu, A.T. (2007), "Alternative plate finite elements for the analysis of thick plates on elastic foundations", *Struct. Eng. Mech., Int. J.*, **26**(1), 69-86. https://doi.org/10.12989/sem.2007.26.1.069
Pabst, W. (2014), "Youngs modulus of isotropic porous materials with spheroidal pores", *J. Eur. Ceram. Soc.*, **34**, 3195-3207. https://doi.org/10.1016/j.jeurceramsoc.2014.04.009
Pabst, W. and Gregorovà, E. (2004a), "Effective elastic properties of alumina-zirconia composite ceramics Part 2. Micromechanical modeling", *Ceramics Silikàty*, **48**, 14-23.
Pabst, W. and Gregorovà, E. (2004b), "Mooney-type relation for the porosity dependence of the effective tensile modulus of ceramics", *J. Mater. Sci.*, **39**, 3213-3215. https://doi.org/10.1023/B:JMSC.0000025863.55408.c9
Pabst, W., Gregorovà, E., Tichà, G. and Tynovà, E. (2004), "Effective elastic properties of aluminazirconia composite ceramicsPart 4. Tensile modulus of porous alumina and zirconia", *Ceramics Silikàty*, **48**, 165-174.
Pabst, W., Gregorovà, E. and Tichà, G. (2006), "Elasticity of porous ceramics: a critical study of modulus porosity relations",

J. Eur. Ceram. Soc., **26**, 1085-1097. https://doi.org/10.1016/j.jeurceramsoc.2005.01.041

Panjehpour, M., Loh, E.W.K. and Deepak, T.J. (2018), "Structural Insulated Panels: State-of-the-Art", *Trends Civil Eng. Architect.*, **3**(1), 336-340. https://doi.org/10.32474/TCEIA.2018.03.000151

Rajabi, J. and Mohammadimehr, M. (2019), "Bending analysis of a micro sandwich skew plate using extended Kantorovich method based on Eshelby-Mori-Tanaka approach", *Comput. Concrete*, *Int. J.*, **23**(5), 361-376. http://doi.org/10.12989/cac.2019.23.5.361

Reddy, J.N. (2000), "Analysis of functionally graded plates", *Int. J. Numer. Method. Eng.*, **47**(1-3), 663-684. https://doi.org/10.1002/(SICI)1097-0207(20000110/30)47:1/3<663::AID-NME787>3.0.CO;2-8

Rezaei, A.S. and Saidi, A.R. (2015), "Exact solution for free vibration of thick rectangular plates made of porous materials", *Compos. Struct.*, **134**, 1051-1060. https://doi.org/10.1016/j.compstruct.2015.08.125

Rezaei, A.S. and Saidi, A.R. (2016), "Application of Carrera unified formulation to study the effect of porosity on natural frequencies of thick porous-cellular plates", *Compos. B*, **91**, 361-370. https://doi.org/10.1016/j.compositesb.2015.12.050

Rezaei, A.S. and Saidi, A.R. (2017), "Buckling response of moderately thick fluid-infiltrated porous annular sector plates", *Acta Mech.*, **228**, 3929-3945. https://doi.org/10.1007/s00707-017-1908-2

Sahoo, B., Sahoo, B., Sharma, N., Mehar, K. and Panda, S.K. (2020), "Numerical buckling temperature prediction of graded sandwich panel using higher order shear deformation theory under variable temperature loading", *Smart Struct. Syst.*, *Int. J.*, **26**(5), 641-656. http://doi.org/10.12989/sss.2020.26.5.641

Saini, R. and Lal, R. (2020), "Axisymmetric vibrations of temperature-dependent functionally graded moderately thick circular plates with two-dimensional material and temperature distribution", *Eng. Comput.* https://doi.org/10.1007/s00366-020-01056-1

Sayyad, A. and Ghumare, S. (2019), "A new quasi-3D model for functionally graded plates", *J. Appl. Computat. Mech.*, **5**(2), 367-380. https://doi.org/10.22055/jacm.2018.26739.1353

Selmi, A. (2020), "Dynamic behavior of axially functionally graded simply supported beams", *Smart Struct. Syst.*, *Int. J.*, **25**(6), 669-678. http://doi.org/10.12989/sss.2020.25.6.669

Selmi, A. and Bisharat, A. (2018), "Free vibration of functionally graded SWNT reinforced aluminum alloy beam", *J. Vibroeng.*, **20**(5), 2151-2164. https://doi.org/10.21595/jve.2018.19445

Shafiei, N., Mousavi, A. and Ghadiri, M. (2016), "On size-dependent nonlinear vibration of porous and imperfect functionally graded tapered microbeams", *Int. J. Eng. Sci.*, **106**, 42-56. https://doi.org/10.1016/j.ijengsci.2016.05.007

Shafiei, N., Mirjavadi, S.S., Mohasel Afshari, B., Rabby, S. and Kazemi, M. (2017), "Vibration of two dimensional imperfect functionally graded (2D-FG) porous nano-/micro-beams", *Comput. Methods Appl. Mech. Eng.*, **322**, 615-632. https://doi.org/10.1016/j.cma.2017.05.007

Shahadat, M.R.B., Alam, M.F., Mandal, M.N.A. and Ali, M.M. (2018), "Thermal transportation behaviour prediction of defective graphene sheet at various temperature: A Molecular Dynamics Study", *Am. J. Nanomater.*, **6**(1), 34-40. https://doi.org/10.12691/ajn-6-1-4

Shen, H-S. (2000), "Nonlinear analysis of simply supported Reissner-Mindlin plates subjected to lateral pressure and thermal loading and resting on two-parameter elastic foundations", *Eng. Struct.*, **23**, 1481-1493. https://doi.org/10.1016/S0141-0296(99)00086-3

Shen, H.S., Yang, J. and Zhang, L. (2001), "Free and forced vibration of Reissner-Mindlin plates with free edges resting on elastic foundations", *J. Sound Vib.*, **244**, 299-320. https://doi.org/10.1006/jsvi.2000.3501

Si, H., Shen, D., Xia, J. and Tahouneh, V. (2020), "Vibration behavior of functionally graded sandwich beam with porous core and nanocomposite layers", *Steel Compos. Struct.*, *Int. J.*, **36**(1), 1-16. http://doi.org/10.12989/scs.2020.36.1.001

Sofiyev, A.H. (2011), "Thermal buckling of FGM shells resting on a two parameter elastic foundation", *Thin-Wall. Struct.*, **49**, 1304-1311. https://doi.org/10.1016/j.tws.2011.03.018

Tayeb, T.S., Zidour, M., Bensattalah, T., Heireche, H., Benahmed, A. and Bedia, E.A. (2020), "Mechanical buckling of FG-CNTs reinforced composite plate with parabolic distribution using Hamilton's energy principle", *Adv. Nano Res.*, *Int. J.*, **8**(2), 135-148. https://doi.org/10.12989/anr.2020.8.2.135

Thanh, C.L., Nguyen, T.N., Vu, T.H., Khatir, S. and Abdel-Wahab, M. (2020), "A geometrically nonlinear size-dependent hypothesis for porous functionally graded micro-plate", *Eng. Comput.* https://doi.org/10.1007/s00366-020-01154-0

Thanh, C.L., Nguyen, K.D., Nguyen, T.N., Khatir, S., Nguyen-Xuan, H. and Abdel-Wahab, M. (2021), "A three-dimensional solution for free vibration and buckling of annular plate, conical, cylinder and cylindrical shell of FG porous-cellular materials using IGA", *Compos. Struct.*, **259**, 113216. https://doi.org/10.1016/j.compstruct.2020.113216

Timesli, A. (2020), "Prediction of the critical buckling load of SWCNT reinforced concrete cylindrical shell embedded in an elastic foundation", *Comput. Concrete*, *Int. J.*, **26**(1), 53-62. http://doi.org/10.12989/cac.2020.26.1.053

Vinyas, M. (2020), "On frequency response of porous functionally graded magneto-electro-elastic circular and annular plates with different electro-magnetic conditions using HSDT", *Compos. Struct.*, **240**, 112044. https://doi.org/10.1016/j.compstruct.2020.112044

Wang, Z.X. and Shen, H.-S. (2013), "Nonlinear dynamic response of sandwich plates with FGM face sheets resting on elastic foundations in thermal environments", *Ocean Eng.*, **57**, 99-110. https://doi.org/10.1016/j.oceaneng.2012.09.004

Winkler, E. (1867), "Die Lehre von der Elastizität and Festigkeit", *Prag. Dominicus*.

Wu, D., Liu, A., Huang, Y., Huang, Y., Pi, Y. and Gao, W. (2018), "Dynamic analysis of functionally graded porous structures through finite element analysis", *Eng. Struct.*, **165**, 287-301. https://doi.org/10.1016/j.engstruct.2018.03.023

Xiang, Y. (2003), "Vibration of rectangular Mindlin plates resting on non-homogenous elastic foundations", *Int. J. Mech. Sci.*, **45**, 1229-1244. https://doi.org/10.1016/S0020-7403(03)00141-3

Yaghoobi, H. and Taheri, F. (2020), "Analytical solution and statistical analysis of buckling capacity of sandwich plates with uniform and non-uniform porous core reinforced with graphene nanoplatelets", *Compos. Struct.*, **252**, 112700. https://doi.org/10.1016/j.compstruct.2020.112700

Yang, B., Ding, H.J. and Chen, W.Q. (2012), "Elasticity solutions for functionally graded rectangular plates with two opposite edges simply supported", *Appl. Math. Model.*, **36**, 488-503. https://doi.org/10.1016/j.apm.2011.07.020

Yang, J., Chen, D. and Kitipornchai, S. (2018), "Buckling and free vibration analyses of functionally graded graphene reinforced porous nanocomposite plates based on Chebyshev-Ritz method", *Compos. Struct.*, **193**, 281-294. https://doi.org/10.1016/j.compstruct.2018.03.090

Yas, M.H. and Tahouneh, V. (2012), "3-D Free vibration analysis of thick functionally graded annular plates on Pasternak elastic foundation via differential quadrature method (DQM)", *Acta. Mech.*, **223**, 43-62. https://doi.org/10.1007/s00707-011-0543-6

Yeghnem, R., Guerroudj, H.Z., Amar, L.H.H., Meftah, S.A., Benyoucef, S., Tounsi, A. and Adda Bedia, E.A. (2017), "Numerical modeling of the aging effects of RC shear walls strengthened by CFRP plates: A comparison of results from

different "code type" models", *Comput*. *Concrete*, *Int*. *J*., **19**(5), 579-588. http://doi.org/10.12989/cac.2017.19.5.579

Yuan, Y., Zhao, K., Zhao, Y. and Kiani, K. (2020), "Nonlocal-integro-vibro analysis of vertically aligned monolayered nonuniform FGM nanorods", *Steel Compos*. *Struct*., *Int*. *J*., **37**(5), 551-569. http://doi.org/10.12989/scs.2020.37.5.551

Zhou, D., Cheung, Y.K., Lo, S.H. and Au, F.T.K. (2004), "Three-dimensional vibration analysis of rectangular thick plates on Pasternak foundation", *Int*. *J*. *Numer*. *Methods*. *Eng*., **59**, 1313-1334. https://doi.org/10.1002/nme.915

Zhu, X., Lu, Z., Wang, Z., Xue, L. and Ebrahimi-Mamaghani, A. (2020), "Vibration of spinning functionally graded nanotubes conveying fluid", *Eng*. *Comput*. https://doi.org/10.1007/s00366-020-01123-7

CC